Transcriptomic evidence for involvement of reactive oxygen species in *Rhizoctonia solani* AG1 IA sclerotia maturation

Bo Liu [1,2] , **Haode Wang** [1] , **Zhoujie Ma** [1] , **Xiaotong Gai** [1] , **Yanqiu Sun** [1] , **Shidao He** [1] , **Xian Liu** [3] , **Yanfeng Wang** [2] , **Yuanhu Xuan** [4] , **Zenggui Gao** Corresp. [1]

1 Institute of Plant Immunology, Shenyang Agricultural University, Shenyang, Liaoning, China
2 College of Life Sciences, Yan'an University, Yan'an, Shanxi, China
3 College of Life Sciences, Shenyang Agricultural University, Shenyang, Liaoning, China
4 College of Plant Protection, Shenyang Agricultural University, Shenyang, Liaoning, China

Corresponding Author: Zenggui Gao
Email address: gaozenggui@syau.edu.cn

Rhizoctonia solani AG1 IA is a soil-borne fungal phytopathogen that can significantly harm crops resulting in economic loss. This species overwinters in grass roots and diseased plants, and produces sclerotia that infect future crops. *R. solani* AG1 IA does not produce spores; therefore, understanding the molecular mechanism of sclerotia formation is important for crop disease control. Toward this end, to identify the genes involved in this process for the development of disease control targets, in this study, the transcriptomes of this species were determined at three important developmental stages (mycelium, sclerotial initiation, and sclerotial maturation) using an RNA-sequencing approach. A total of 5016, 6433, and 5004 differentially expressed genes (DEGs) were identified in the sclerotial initiation vs. mycelial, sclerotial maturation vs. mycelial, and sclerotial maturation vs. sclerotial initiation stages, respectively. Moreover, Gene Ontology (GO) and Kyoto Encyclopedia of Genes and Genomes (KEGG) analyses showed that these DEGs were enriched in diverse categories, including oxidoreductase activity, carbohydrate metabolic process, and oxidation-reduction processes . Twelve DEGs were further verified using reverse transcription quantitative PCR (RT-qPCR). Among the genes examined, NADPH oxidase 1 (*NOX1*) and superoxide dismutase (*SOD*) were highly induced in the stages of sclerotial initiation and maturation. In addition, the highest reactive oxygen species (ROS) production levels were detected during sclerotial initiation, and enzyme activities of NOX1, SOD, and catalase (CAT) matched with the gene expression profiles. To further evaluate the role of ROS in sclerotial formation , *R. solani* AG1 IA was treated with the CAT inhibitor aminotriazole and H_2O_2, resulting in the early differentiation of sclerotia . Taken together, this study provides useful information toward understanding the molecular basis of *R. solani* AG1 IA sclerotial formation and maturation, and identified the important role of ROS in these processes.

1 **Transcriptomic evidence for involvement of reactive oxygen**

2 **species in *Rhizoctonia solani* AG1 IA sclerotia maturation**

4 Bo Liu[1][2], Haode Wang[1], Zhoujie Ma[1], Xiaotong Gai[1], Yanqiu Sun[1], Shidao He[1], Xian Liu[3], Yanfeng Wang[2], Yuan

5 Hu Xuan[4], Zenggui Gao[1]

6 [1] Institute of Plant Immunology, Shenyang Agricultural University, Shenyang, Liaoning, China

7 [2] College of Life Sciences, Yan'an University, Yan'an, Shanxi, China

8 [3] College of Life Sciences, Shenyang Agricultural University, Shenyang, Liaoning, China

9 [4] College of Plant Protection, Shenyang Agricultural University, Shenyang, China

11 Corresponding Author:

12 Zenggui Gao

13 Shenyang Agricultural University, Shenyang, Liaoning 110866, China

14 Email address: gaozenggui@syau.edu.cn

ABSTRACT

Rhizoctonia solani AG1 IA is a soil-borne fungal phytopathogen that can significantly harm crops resulting in economic loss. This species overwinters in grass roots and diseased plants, and produces sclerotia that infect future crops. *R. solani* AG1 IA does not produce spores; therefore, understanding the molecular mechanism of sclerotia formation is important for crop disease control. Toward this end, to identify the genes involved in this process for the development of disease control targets, in this study, the transcriptomes of this species were determined at three important developmental stages (mycelium, sclerotial initiation, and sclerotial maturation) using an RNA-sequencing approach. A total of 5016, 6433, and 5004 differentially expressed genes (DEGs) were identified in the sclerotial initiation vs. mycelial, sclerotial maturation vs. mycelial, and sclerotial maturation vs. sclerotial initiation stages, respectively. Moreover, Gene Ontology (GO) and Kyoto Encyclopedia of Genes and Genomes (KEGG) analyses showed that these DEGs were enriched in diverse categories, including oxidoreductase activity, carbohydrate metabolic process, and oxidation-reduction processes. Twelve DEGs were further verified using reverse transcription quantitative PCR (RT-qPCR). Among the genes examined, NADPH oxidase 1 (*NOX1*) and superoxide dismutase (*SOD*) were highly induced in the stages of sclerotial initiation and maturation. In addition, the highest reactive oxygen species (ROS) production levels were detected during sclerotial initiation, and enzyme activities of NOX1, SOD, and catalase (CAT) matched with the gene expression profiles. To further evaluate the role of ROS in sclerotial formation, *R. solani* AG1 IA was treated with the CAT inhibitor aminotriazole and H_2O_2, resulting in the early differentiation of sclerotia. Taken together, this study provides useful information toward understanding the molecular basis of *R. solani* AG1 IA sclerotial formation and maturation, and identified the important role of ROS in these processes.

INTRODUCTION

Rhizoctonia solani is a soil-borne pathogen belonging to the class Agaricomycetes, family Ceratobasidiaceae that causes various plant diseases and attacks crops (maize, potatoes, rice, and soybean). *R. solani* is classified into 14 anastomosis groups (AG 1–13 and AG 1 IB) (Ogoshi 1987; Priyatmojo et al. 2001). Maize sheath blight is one of the most serious and widely distributed diseases caused by *R. solani* AG1 IA, resulting in severe yield losses in maize-cultivating areas worldwide. The sclerotium is a special structure of *R. solani* that overwinters in the soil or diseased plants, and can survive under adverse conditions (e.g., low temperature) for long periods (Rush & Lee 1983; Boland et al. 2004). Although sheath blight disease-resistant varieties of maize are available, these varieties are limited; thus, treating maize with fungicides remains the main approach to control the spread of *R. solani* in crops (Zhao et al. 2006). However, the emergence of fungicide tolerance has now made it even more difficult to control this disease. Since *R. solani* AG1 IA does not produce spores, the growth and germination of sclerotial are the key to maintaining the life of *R. solani*.

In 1954, Townsend and Willetts divided the development of sclerotia into three stages: initiation, development, and maturation. The initiation stage is marked by the appearance of the

55 sclerotium with white aerial mycelia entangled around the edges of the culture medium. In the
56 development stage, the sclerotium becomes further entangled and increases in size along with
57 secretion of a clear or tan-colored liquid on the surface. The maturation phase involves the
58 accumulation of melanin in epidermal cells, and internal hardening. (Townsend and Willetts
59 1954). Substrates associated with these stages (initiation, development, and maturation) of a
60 typical spherical sclerotium in filamentous fungi may show a differentiated structure, which can
61 possibly insulate itself from environmental oxygen (Georgiou et al. 2006). One of the most
62 unique features of the sclerotium is that it becomes inactive when the environmental conditions
63 are not conducive for growth. In the mature stage of the sclerotium, it can survive for many years
64 enduring extreme temperatures, desiccation, starvation, harmful irradiation, and biological
65 degradation (Georgiou et al. 2006; Liang et al. 2010). Thus, understanding how the sclerotia
66 form is important for crop disease control. However, the molecular mechanisms of sclerotia
67 formation of *R. solani* have been poorly understood.
68 Therefore, to understand the molecular basis of sclerotia formation, we determined the
69 transcriptomes of *R. solani* AG1-IA in the three important developmental stages (mycelium,
70 sclerotia initiation, and sclerotia maturation) using RNA-sequencing (RNA-seq), which has been
71 frequently applied to the discovery of the molecular mechanisms underlying pathogenic growth
72 and development (Egan et al. 2012; Metzker 2010; O'Connell et al. 2012). Moreover, RNA-seq
73 performs better DEG analysis compared to other high-throughput technologies (Wang et al.
74 2009). Transcriptome data were collected from the mycelium (4 d of growth), initial sclerotia (5
75 d of growth), and mature sclerotia (7 d of growth) of *R. solani* AG1-IA. Moreover, we examined
76 the underlying pathways involved in sclerotonium formation. In particular, we tested the
77 hypothesis that ROS are involved in the process.
78 ROS arises from mitochondrial oxidative metabolism and in the cellular response to
79 xenobiotics, cytokines, and bacterial invasion. (Ray et al. 2012). The influence of ROS on
80 molecular and biochemical processes as well as signal transduction pathways is well-established,
81 which in turn affects cell proliferation and differentiation, leading to the death of fungi andother
82 organisms (Allen & Tresini 2000). ROS are more reactive than O_2 in its ground state or triplet
83 state ($^3O_2$). These ROS are dioxygen molecules in their excited singlet state forms ($^1O_2$) and
84 partially reduced forms of oxygen, including superoxide radical ion and its protonated forms HO.
85 2, hydroxyl radical (HO·), and hydrogen peroxide (H_2O_2) (Cui et al. 2011; Georgiou et al. 2006;
86 Turrens 2003). Moreover, ROS play an important role in the regulation of cellular signaling
87 pathways; for example, hyperoxidant states are the primary driving force for cell differentiation
88 (Fang et al. 2002; Lara-Ortíz et al. 2003). Chet and Henis (1975) first proposed that the
89 formation of sclerotia requires the participation of oxygen. However, addition of a hydroxyl
90 radical scavenger to the culture medium of *Sclerotinia sclerotiorum* and *R. solani* was shown to
91 suppress sclerotium formation (Georgiou et al. 2000). Therefore, to further understand this
92 process, we measured the production of ROS during the three stages of sclerotium formation and
93 determined the activities of key ROS- producing and ROS-scavenging enzymes during the
94 process.
95 This work should help to identify the critical genes responsible for formation of the sclerotium

96 of *R. solani* AG1-IA in maize toward understanding the underlying molecular mechanism. The
97 generated results should provide a scientific foundation for the development of new strategies
98 and targets toward the prevention of corn sheath blight.

MATERIALS AND METHODS

Sample collection and preparation

101 *R. solani* AG1-IA were collected from the Institute of Plant Immunology at Shenyang
102 Agricultural University. This strongly pathogenic strain was screened as previously described
103 (Tingting et al. 2013) and cultivated on potato dextrose agar (PDA), at a temperature of 26°C.
104 The *R. solani* AG1-IA were collected from PDA at different stages of maturation: mycelium,
105 RWF9M (4 d of growth); sclerotial initiation, RWF9SI (5 d of growth); sclerotial maturation,
106 RWF9S (7 d of growth) (Fig. 1). *R. solani* AG1-IA obtained were stored at -80°C. Three mycelia
107 growth plates were used as three biological replicates for sclerotia formation and harvesting.

RNA quantification

109 RNA was extracted at the three developmental stages of the sclerotium (mycelium, sclerotium
110 initiation, and sclerotium maturation) using TaKaRa MiniBEST Universal RNA Extraction Kit
111 (TaKaRa, Shiga, Japan). RNA quality was assessed on 1% agarose gel. PrimeScript™ RT
112 reagent kit with gDNA Eraser (Takara, Shiga, Japan) was used to synthesize the cDNA. Total
113 RNA was treated with DNase to remove gDNA.

Library preparation for transcriptome sequencing

115 This study provided 3 μg RNA per sample for on-machine sequencing, performed using a
116 NEBNext® Ultra™ RNA Library Prep Kit for Illumina® (New England Biolabs, USA). Using
117 mRNA as a template, first-strand cDNA was synthesized using random hexamers, followed
118 synthesize and purify second-strand cDNA. The purified second-strand cDNA was subjected to
119 terminal repair. A tail was added, and the sequencing adapter was adaptor-ligated cDNA. Then,
120 we produced the cDNA library by fragment size selection (150-200 bp).

Clustering and sequencing

122 In the cBot Cluster Generation, the samples were clustered using the TruSeq PE Cluster Kit v3-
123 cBot-HS (Illumina); after clustering, the library was sequenced to generate 125 bp/150 bp paired-
124 end reads on the Illumina HiSeq platform. All raw-sequence read were stored at Sequence Read
125 Archive (SRP134130).

Quality control

127 The raw sequence obtained by sequencing contains low-quality reads with linkers. The low-
128 quality reads and the reads with adapter or poly-N were removed from raw data. Then, we
129 counted the quality-control indices (Q20, Q30) and GC content (Trapnell et al. 2010).

Read mapping to the reference genome

We used TopHat v2.0.12 and aligned the clean reads with those from *Rhizoctonia solani* AG-3 Rhs1AP genome (Cubeta et al. 2014) (Trapnell et al. 2009).

Quantification of gene expression levels

HTSeq v0.6.1 software was used to analyze the gene expression level in each sample. The fragments per kilobase of transcript per million reads (FPKM) value of each gene was then calculated based on the length and depth (Trapnell et al. 2010).

Differential expression analysis

We used the DESeq R software package (1.18.0) to analysis DEGs of the three stages (3 replicates per stage) (Wang et al. 2009). The P values of differentially expressed genes were adjusted by Benjamin and Hochberg methods (P values < 0.05) (Anders & Huber 2012; Benjamini & Hochberg 1995).

GO and KEGG analysis

We used GO seq R package for correcting gene (P-value < 0.05) and implemented GO enrichment analysis of DEGs (Young et al. 2010). We used KOBAS to analyse the KEGG of DEGs (Kanehisa et al. 2007; Mao et al. 2005).

Determination of ROS production

ROS generation in the mycelium, initial sclerotium, and mature sclerotium of *R. solani* AG1 IA was detected using dichloro-dihydrofluorescein diacetate (H$_2$DCFDA) (Ezaki et al. 2000). Samples from the three stages were incubated with 100 μL of 10 μM H$_2$DCFDA, for 90 min. To indicate the extent of ROS production, the fluorescence staining intensity was evaluated by using a fluorescent enzyme labeling instrument SpectraMax Gemini®EM (Molecular Devices, USA) at an excitation wavelength of 488 nm and emission wavelengths of 530 nm.

Enzyme activity assays

SOD enzyme activity was measured based on the method by Beauchamp et al. (1971) with minor modifications. To 100 mg of fungi, 1 mL sodium phosphate buffer (60 mM, pH 7.0) was added. The mixture was grinded to extract SOD. The activity of the SOD enzyme was determined by adding nitroblue tetrazolium (NBT) and measuring absorbance at 560 nm (Beauchamp et al. 1971). CAT enzyme activity was measured based on the method by Khanam et al. (2005) with minor modifications. To 100 mg of fungi, 1 mL buffer (16.6 mM sodium phosphate buffer (pH 7.2), 0.6 mM EDTA, and 50 mg PVP) was added and the mixture was grinded to extract CAT. The rate of consumption of hydrogen peroxide by the extract was assayed by measuring absorbance at 240 nm. Next, cell membranes were separated from fungi by two-phase partitioning (Qiu et al. 2002). The superoxide radicals in the membrane were determined by

164   treatment with 0.5 mM XTT and 50 mM NADPH followed by measurement of absorbance at
165   470 nm. Thus, the total NOX enzyme activity was calculated (Able et al. 1998, Sutherland et al.
166   1997). All enzyme assays were performed in triplicates with two repetitions.

167   **Real-time PCR analysis**

168   Twelve specific primers and four reference gene-specific primers were obtained (Table S1). The
169   amplification efficiency of primer pairs was determined as described by Radonić et al. (2004).
170   Twelve DEGs were selected for RT-qPCR confirmation. The reaction mixture comprised 10 μL
171   SYBR (TaKaRa, Shiga, Japan), 2 μL cDNA, 2 μL primer pair, and 6 μL water. The reaction was
172   performed on a CFX-96 system (BioRad, USA). All samples were tested in triplicates with two
173   repetitions. Mapping was performed by using SigmaPlot 12.5. We used geNorm, BestKeeper,
174   NormFinder, and the deltaCt method to evaluate four candidate reference genes in three stages
175   (Andersen et al. 2004, Vandesompele et al. 2002, Pfaffl et al. 2004, Silver et al. 2006) (Table
176   S2).

177   **RESULTS**

178   **Transcriptome sequencing reads quality inspection and sample correlation analysis during**
179   **sclerotia formation of *R. solani* AG1 IA**

180   Total RNAs were isolated from RWF9M (mycelium), RWF9SI (sclerotial initiation), and
181   RWF9S (sclerotial maturation) (Fig. 1). From three biological replicates, sequences of nine
182   samples were generated to achieve 477,763,884 raw reads, ranging from 45.44 to 65.77 million
183   reads per sample. After quality filtering, 462,318,502 clean reads remained, ranging between
184   44.15 and 63.84 million per sample. Based on the quality test of the clean reads (Table 1), the
185   Q20 from all reads was between 95.87% and 97.12% while the Q30 was between 90.79% and
186   92.35%. These results showed that the data quality of the transcriptome was high and suitable for
187   transcriptome analysis. The use of triplicates was employed for each biological sample on the
188   data of original reads for the correlation test.
189   Prior to the DEGs analysis, the pearson correlation coefficients between samples were
190   determined by RNA-seq correlation analysis. As shown in Figure 2A, the
191   Pearson correlation coefficient of each sample was over 0.90, demonstrating good repeatability.
192   The results of the RPKM distribution were showed in Fig. 2B and RPKM density distribution
193   were showed in Fig. 2C.

194   **DEGs during sclerotia formation of *R. solani* AG1 IA**

195   To obtain the DEGs, the gene expression of sclerotial initiation and maturation were compared to
196   the mycelial stage. In addition, the sclerotial maturation was compared to the sclerotial initiation
197   stage. A total of 5016, 6433, and 5004 DEGs were identified in the sclerotial initiation vs.
198   mycelial, sclerotial maturation vs. mycelial, and sclerotial maturation vs. sclerotial initiation
199   comparisons, respectively (Fig. 3). A total of 276, 1229, and 614 DEGs were identified in the
200   sclerotial initiation vs. mycelial, sclerotial maturation vs. mycelial, and sclerotial maturation vs.

201 sclerotial initiation groups, respectively (Fig. 3A). Overall, 2381 and 2635 genes were
202 upregulated and downregulated, respectively, between the sclerotial initiation and mycelial
203 samples. In the volcano plot, a total of 2381, 3102, and 2505 DEGs were upregulated in
204 sclerotial initiation vs. mycelial, sclerotial maturation vs. mycelial, and sclerotial maturation vs.
205 sclerotial initiation comparisons, respectively. In contrast, a total of 2635, 3331, and 2499 DEGs
206 were downregulated in sclerotial initiation vs. mycelial, sclerotial maturation vs. mycelial, and
207 sclerotial maturation vs. sclerotial initiation comparisons, respectively.
208   Under the GO terms, the unigenes were found to be involved in molecular function, cellular
209 component, and biological process. Interestingly, the number of unigenes associated with the
210 ribosome was particularly high in all three comparisons (Fig. 4). For the GO terms of DEGs in
211 the sclerotial initiation vs. mycelial group, the high number of unigenes associated with single-
212 organism metabolic, metabolic, and oxidation-reduction (Fig. 4). The sclerotial maturation vs.
213 mycelial group were largely associated with biological process, metabolic process,
214 oxidoreductase activity, and catalytic activity. In addition, the DEGs in the sclerotial maturation
215 vs. sclerotial initiation group were largely associated with carbohydrate metabolic process,
216 cellular protein metabolic process, phosphorus metabolic process, and structural molecule
217 activity.
218   When the DEGs were searched against the KEGG pathway, 2185 (sclerotial initiation vs.
219 mycelial), 2286 (sclerotial maturation vs. mycelial), and 1882 (sclerotial maturation vs. sclerotial
220 initiation) DEGs with significant hits were returned. The top 20 pathways in three groups are
221 listed (Table 2, Table 3, and Table 4). Cluster analysis (Fig. 5) revealed that the expression
222 pattern for DEGs in sclerotial initiation and maturation differ from that of the mycelial stage,
223 indicating a significant change in gene expression levels during sclerotia formation. Eight
224 clusters were plotted with their expression patterns (Fig. 5A). Based on the obtained FPKM data
225 for hierarchical cluster analysis (Fig. 5B). As shown in Figure 5, subcluster 1 included 2334
226 genes with down-regulated expression at both sclerotia stages, and the expression levels of these
227 genes were slightly lower in the sclerotial initiation and maturation samples than those in the
228 mycelial samples. The 1396 genes in subcluster 2 were up-regulated at the sclerotial initiation
229 stage compared to the mycelial stage, and then down-regulated at the sclerotial stage in
230 comparison to the sclerotial initiation stage. The 220 genes in subcluster 3 were down-regulated
231 in both sclerotial stages, the expression levels in sclerotial maturation were lower than the other
232 two stages. Subcluster 4 included 570 genes with up-regulated expression in both stages.
233 Subcluster 5 included 2511 genes with higher expressionin sclerotial maturation than in the other
234 two stages. Subcluster 6 included 922 genes with higher expression in the mycelial stage than in
235 the two sclerotial stages. Subcluster 7 included 586 genes with higher expression in the sclerotial
236 initiation stage than the other two stages. The 26 genes in subcluster 8 were up-regulated at both
237 stages, and the expression levels in sclerotial initiation were higher than those in the mycelial
238 stage, whereas those of the sclerotial maturation stage were lower compared to the sclerotial
239 initiation stage. The top 20 genes from each category were selected (Tables S3–S10), indicating
240 that NADPH dehydrogenase, cytochrome P450, oxygen-dependent choline dehydrogenase,
241 chitin synthase, O-methylsterigmatocystin oxidoreductase, CAT, and NADPH-P450 reductase

242   play particularly important roles in sclerotial formation. The DEGs of each category were
243   annotated in GO terms and searched against the KEGG pathway (Fig. S1, S2). The GO
244   classification showed that a higher proportion of DEGs in subcluster 3, 4, and 8 are involved in
245   oxidation-reduction process, oxidoreductase activity, and antioxidant activity. In subcluster 4,
246   four genes (*SOD*, *CAT*, putative protein disulfide-isomerase, and glutathione peroxidase) were
247   classified in the antioxidant activity GO term, and *SOD* and *CAT* were predicted to be localized
248   at the peroxisome.

249   **Oxidative stress responses**

250   To investigate the changes of ROS production during the formation of sclerotia, and changes of
251   enzymes in ROS, the fluorescent dye H_2DCFDA was used to measure intracellular ROS levels in
252   the three stages of *R. solani* AG1 IA development. As shown in Figure 6, ROS were detected in
253   all three stages, although the intensity of fluorescence was much higher in the sclerotial initiation
254   stage compared to the other two stages.
255   CAT, SOD, and NOX are the key to the production and removal of ROS in the formation of
256   sclerotia. Therefore, we assayed these enzymes. NOX and SOD showed an initial increase in
257   activity followed by a decrease. NOX enzymes participates in the production of superoxide, an
258   important precursor of ROS, and SOD can convert superoxide radicals to hydrogen peroxide.
259   Thus, the increase of NOX and SOD enzyme activities in the sclerotial initiation showed that the
260   ROS level improved. By contrast, CAT activity decreased in all three stages, which indicates a
261   reduction of ROS scavenging (Fig. 6). In addition, we treated the samples with the CAT inhibitor
262   aminotriazole along with H_2O_2, and monitored sclerotial formation, which showed that H_2O_2
263   accumulation in the absence of CAT led to the early differentiation of sclerotia (Fig. S3, S4).

264   **Amplification specificity and efficiency**

265   The gel agarose results showed all primer bands at a single size range of 100-300 bp, and the
266   melting curves had a single peak (Fig. S5-S9). The PCR efficiency (E) of all the primers was
267   94.9-109.5%, and the correlation coefficients (R^2) were greater than 0.982 (Table S1). These
268   results indicated that all primers could be used for subsequent RT-qPCR. Four reference genes
269   were ranked by their average expression stability (M-value), as shown in Table S2.
270   Comprehensive analysis showed that 18sRNA was more stable compared with the RNA of actin,
271   β-tubulin (*TUB*), and glyceraldehyde-3-phosphate dehydrogenase (*GAPDH*).

272   **Validation of gene expression level changes during sclerotia formation of *R. solani* AG1 IA**
273   **by RT-qPCR**

274   The relative mRNA levels of 12 DEGs among the three stages were analyzed using RT-qPCR: 6-
275   phosphogluconate dehydrogenase (*6PGD*), galactinol synthase 7 (*CLOS7*), glucan 1,3-beta-
276   glucosidase, beta-galactosidase, NADH dehydrogenase, NADPH-P450 reductase, obtusifoliol
277   14-alpha demethylase (*CYP51*), *SOD*, *NOX*, oxygen-dependent choline dehydrogenase (*bETA*),
278   chitin synthase D, and phosphoadenosine phosphosulfate reductase (*MET16*). The expression
279   level trends of most of these genes were consistent between the RNA-seq and RT-qPCR results

280 (Fig. 7).

281 **DISCUSSION**

282 As far as we know, this is the first transcriptome analysis on maize sheath blight (*R. solani* AG1
283 IA) during the sclerotium formation process. Kwon et al. (2014) analyzed proteomic changes
284 during the process of sclerotial formation of *R. solani* for 5 days, 7 days, and 10 days,
285 respectively, and obtained 55 differentially expressed proteins, representing high expression of
286 processing, cellular processes, amino acid metabolism, cell defense, and carbohydrate
287 metabolism during the sclerotium formation. In line with these previous findings, through RNA-
288 seq analysis during the formation of the sclerotium, we identified 5000–6000 DEGs between the
289 three stages from the mycelial stage to the sclerotial initiation and maturation stages, and the
290 majority of the highly expression were involved in the oxidation-reduction process, carbohydrate
291 metabolic process, catalytic activity, and oxidoreductase activity. The involvement of
292 carbohydrate metabolism suggests thatcarbon sources are quickly consumed in sclerotial
293 maturation. Therefore, the cell metabolism was reduced. In addition, six antioxidant enzymes
294 (three SODs, dihydropteroate synthase, cytochrome C peroxidase, and alpha-ketoglutarate-
295 dependent taurinedioxygenase) of *R. solani* were differently expressed during sclerotial
296 maturation (Kwon et al. 2014). In this study, SOD, dihydropteroate synthase, and cytochrome C
297 peroxidase were found to be differentially expressed among all three stages, and more
298 antioxidant genes were found to accumulate during the sclerotia formation process, including
299 CAT, putative protein disulfide-isomerase, and glutathione peroxidase. These results showed that
300 SOD and CAT may regulate ROS levels to maintain cellular redox homoeostasis within cells
301 during sclerotial maturation.
302 Zheng et al. (2013) suggested that in traditional breeding strategies, no crops have high
303 resistance to *R. solani.* Although some resistance traits have been found in rice and maize, no
304 resistance genes have been identified and cloned. However, these authors fully sequenced the
305 transcriptome of *R. solani* AG1 IA, providing a molecular basis for the breeding of rice plants
306 with resistance to the disease (Zheng et al. 2013). Our present work thus largely expands the
307 available tools for breeding disease-resistant maize through generation of a transcriptome library
308 of the sclerotial maturation of *R. solani* AG1 IA.
309 Some genes have previously been linked to sclerotia formation. *R. solani* with knockout G-
310 protein α subunit showed a change in morphology, and the ability to form sclerotium was
311 completely lost (Charoensopharat K et al. 2008). The osmotic stress response and microsclerotia
312 formation of *Verticillium dahliae* were regulated by the mitogen-activated protein kinase gene
313 (VdHog1) (Yonglin et al. 2016). We further identified a large number genes related to sclerotia
314 formation using RNA-seq technology. Moreover, the cluster analysis revealed that the
315 expression pattern of DEGs in the sclerotial initiation and maturation stages differed from that in
316 the mycelial stage. Eight clusters were plotted with their expression patterns, revealing
317 significant difference of previously identified sclerotial formation-related genes. In particular,
318 subcluster 4 included 570 genes that were up-regulated in both sclerotia stages, which were
319 highly enriched in GO terms related to peroxidase activity, oxidoreductase activity, and

320   oxidation-reduction process, and KEGG pathways of peroxisome, glutathione metabolism,
321   ascorbate, and aldarate metabolism. This suggests that antioxidants (e.g., glutathione, vitamin E,
322   and ascorbic acid,) and enzymes (e.g., SOD, CAT) can change the balance of ROS and thus
323   affect sclerotial formation.

324   Under hyperoxidant state, cells can be transformed between differentiated and undifferentiated
325   states, and the ROS level is higher than that in antioxidation. In this state, the cells need to
326   prevent premature entry into the hyperoxidant state. To prevent entry into this hyperoxidant
327   state, cells via cell aggregation or fusion in the biogenesis of sclerotia, plasmodia, and sex organs
328   (Georgiou et al. 2006). Moreover, we found that SOD and NOX activities were particularly high
329   in the initiation stages, suggesting that the early developmental stage of sclerotium generates
330   ROS in hyperoxidant state. In contrast, CAT activity decreased in the maturation stage,
331   suggesting an increase in the consumption of oxygen molecules with a consequent blockage of
332   oxygen molecules from entering the cells to balance the peroxide content. Thus, ROS is an
333   important inducing factor for the growth of *R. solani* from the mycelium to sclerotium.

334   NOX1, SOD, CAT are considered to be involved in superoxide anion generation, fungal
335   growth, and cell differentiation (Peraza & Hansberg 2002; Georgiou et al. 2006). Kim et al.
336   (2011) silenced NOX genes in *S. sclerotiorum, SsNOX1* and *SsNOX2*, and found that the
337   production of ROS among the mutant strains decreased, sclerotia could not be formed, and the
338   synthesis of oxalic acid—an important pathogenic factor—also decreased significantly. Although
339   the pathogenicity of the mutant was also significantly weakened, the gene silencing largely
340   affected the formation of sclerotia rather than the pathogenicity of *S. sclerotiorum*. Furthermore,
341   the mutation caused increased sensitivity to oxidative stress and significantly reduced the risk of
342   disease (Veluchamy et al. 2012). Overall, our transcriptome analysis identified that changes in
343   the expression of ROS-related genes, *NOX1*, *SOD*, and *CAT*, are key events during sclerotia
344   formation and development. These findings were confirmed with RT-qPCR validation for 12
345   genes, including *MET16*, *6PGD,* and *CLOS7* in addition to *NOX1*, *SOD,* and *CAT*, which may be
346   involved in the production of superoxide anions, fungal growth, and cell differentiation. Thus,
347   this study provides molecular-level evidence that active oxygen plays a role in *R. solani* AG1 IA
348   sclerotia maturation, offering further insight into the molecular mechanism of sclerotial
349   development.

350   **CONCLUSIONS**

351   In this study, we found a total of 8567 DEGs throughout *R. solani* AG1 IA sclerotial maturation,
352   which were largely associated with oxidoreductase activity, carbohydrate metabolic process, and
353   oxidation-reduction process. Cluster analysis revealed that genes showing the same trend in
354   expression changes during sclerotia formation may have the same function. Twelve of these
355   DEGs were confirmed using RT-qPCR, including *NOX1*, *SOD*, and *CAT*, demonstrating a key
356   role of oxidative stress through the production of superoxide anions, as well as general
357   associations with fungal growth and cell differentiation. Based on our results, further studies
358   should be performed to elucidate the specific metabolic pathways and functions during sclerotial
359   development using modern techniques. The genes identified in this work only present the first

360 step in revealing the underlying processes, but should provide a useful resource and targets for
361 developing strategies toward the prevention and control of diseases caused by *R. solani* AG1 IA
362 to improve crop productivity.

363 **Supplemental information**

364 Supplemental Tables all supplemental tables (Table S1-S10).
365 Supplemental Figures all supplemental figures (Figure S1-S10).

366 **REFERENCES**

367 **Able AJ, Guest DI, Sutherland MW. 1998.** Use of a new tetrazolium-based assay to study the
368   production of superoxide radicals by tobacco cell cultures challenged with avirulent
369   zoospores of Phytophthora parasitica var nicotianae. *Plant Physiology*. **117:**491–499.
370   DOI 10.1104/pp.117.2.491.
371 **Allen R, and Tresini M. 2000.** Oxidative stress and gene regulation. *Free Radical Biology and*
372   *Medicine* **28:**463-499. DOI 10.1016/S0891-5849(99)00242-7.
373 **Anders S, and Huber W. 2012.** Differential expression of RNA-Seq data at the gene level–the
374   DESeq package. *Heidelberg, Germany: European Molecular Biology Laboratory*.
375   Available at https://core.ac.uk/display/23260267 (accessed 30 September 2013)
376 **Andersen CL, Jensen JL, Orntoft TF. 2004.** Normalization of real-time quantitative reverse
377   transcription-PCR data: a modelbased variance estimation approach to identify genes
378   suited for normalization, applied to bladder and colon cancer data sets. *Cancer Research*
379   **64:**5245–5250. DOI 10.1158/0008-5472.CAN-04-0496.
380 **Beauchamp C, Fridovich I. 1971.** Superoxide dismutase: improved assays and an assay
381   applicable to acrylamide gels. *Analytical Biochemistry* **44:**276-287. DOI 10.1016/0003-
382   2697(71)90370-8.
383 **Benjamini Y, and Hochberg Y. 1995.** Controlling the false discovery rate: a practical and
384   powerful approach to multiple testing. *Journal of the royal statistical society* **57:**289-300.
385   DOI 10.2307/2346101.
386 **Boland G, Melzer M, Hopkin A, Higgins V, and Nassuth A. 2004.** Climate change and plant
387   diseases in Ontario. *Canadian Journal of Plant Pathology* **26:**335-350. DOI
388   10.1080/07060660409507151.
389 **Charoensopharat K, Aukkanit N, Thanonkeo S, Saksirirat W, Thanonkeo P, Akiyama K.**
390   **2008.** Targeted disruption of a G protein α subunit gene results in reduced growth and
391   pathogenicity in *Rhizoctonia solani*. *World Journal of Microbiology & Biotechnology*
392   **24:**345-351. DOI 10.1007/s11274-007-9476-6.
393 **Chet I, and Henis Y. 1975.** Sclerotial morphogenesis in fungi. *Annual review of phytopathology*
394   **13:**169-192. DOI 10.1146/annurev.py.13.090175.001125.
395 **Cubeta MA, Thomas E, Dean RA, Jabaji S, Neate SM, Tavantzis S, Toda T, Vilgalys R,**
396   **Bharathan N, Fedorova-Abrams N, Pakala SB, Pakala SM, Zafar N, Joardar V,**
397   **Losada L, Nierman WC. 2014.** Draft genome sequence of the plant-pathogenic soil
398   fungus *Rhizoctonia solani* anastomosis group 3 strain Rhs1AP. *Genome Announcements*

399   **5**:e1072-14. DOI 10.1128/genomeA.01072-14.

400   **Cui H, Kong Y, and Zhang H. 2011.** Oxidative stress, mitochondrial dysfunction, and aging.
401   *Journal of signal transduction* **2012:** 646354. DOI 10.1155/2012/646354.

402   **Egan AN, Schlueter J, and Spooner DM.** 2012. Applications of next-generation sequencing in
403   plant biology. *Botanical Soc America* **99:** 175-185. DOI 10.3732/ajb.1200020.

404   **Ezaki B, Gardner RC, Ezaki Y, Matsumoto H. 2000.** Expression of aluminum-induced genes
405   in transgenic arabidopsis plants can ameliorate aluminum stress and/or oxidative stress.
406   *Plant Physiology* **122:**657–665. DOI 10.1104/pp.122.3.657.

407   **Fang G-C, Hanau R, and Vaillancourt L. 2002.** The SOD2 gene, encoding a manganese-type
408   superoxide dismutase, is up-regulated during conidiogenesis in the plant-pathogenic
409   fungus Colletotrichum graminicola. *Fungal Genetics and Biology* **36:**155-165. DOI
410   10.1016/S1087-1845(02)00008-7.

411   **Georgiou CD, Patsoukis N, Papapostolou I, and Zervoudakis G. 2006.** Sclerotial
412   metamorphosis in filamentous fungi is induced by oxidative stress. *Integrative and*
413   *comparative Biology* **46:**691-712. DOI 10.1093/icb/icj034.

414   **Georgiou CD, Tairis N, and Sotiropoulou A. 2000.** Hydroxyl radical scavengers inhibit
415   sclerotial differentiation and growth in *Sclerotinia sclerotiorum* and *Rhizoctonia solani*.
416   *Mycological Research* **104:**1191-1196. DOI 10.1017/S0953756200002707.

417   **Kanehisa M, Araki M, Goto S, Hattori M, Hirakawa M, Itoh M, Katayama T, Kawashima**
418   **S, Okuda S, and Tokimatsu T. 2007.** KEGG for linking genomes to life and the
419   environment. *Nucleic acids research* **36:**D480-D484. DOI 10.1093/nar/gkm882.

420   **Khanam NN, Ueno M, Kihara J, Honda Y, Arase S. 2005.** Suppression of red light-induced
421   resistance in broad beans to Botrytis cinerea by salicylic acid. *Physiological & Molecular*
422   *Plant Pathology* **66:**20-29. DOI 10.1016/j.pmpp.2005.03.006.

423   **Kim H-j, Chen C, Kabbage M, and Dickman MB. 2011.** Identification and characterization of
424   *Sclerotinia sclerotiorum* NADPH oxidases. *Applied and environmental microbiology*
425   **77:**7721-7729. DOI 10.1128/AEM.05472-11.

426   **Kwon YS, Kim SG, Chung WS, Bae H, Jeong SW, Shin SC, Jeong M-J, Park S-C, Kwak**
427   **Y-S, and Bae D-W. 2014.** Proteomic analysis of *Rhizoctonia solani* AG-1 sclerotia
428   maturation. *Fungal biology* **118:**433-443. DOI 10.1016/j.funbio.2014.02.001.

429   **Lara-Ortíz T, Riveros-Rosas H, and Aguirre J. 2003.** Reactive oxygen species generated by
430   microbial NADPH oxidase NoxA regulate sexual development in *Aspergillus nidulans*.
431   *Molecular microbiology* **50:**1241-1255. DOI 10.1046/j.1365-2958.2003.03800.x.

432   **Liang Y, Rahman MH, Strelkov SE, and Kav NN. 2010.** Developmentally induced changes in
433   the sclerotial proteome of *Sclerotinia sclerotiorum*. *Fungal biology* **114:**619-627. DOI
434   10.1016/j.funbio.2010.05.003.

435   **Mao X, Cai T, Olyarchuk JG, and Wei L. 2005.** Automated genome annotation and pathway
436   identification using the KEGG Orthology (KO) as a controlled vocabulary.
437   *Bioinformatics* **21:**3787-3793. DOI 10.1093/bioinformatics/bti430.

438   **Metzker ML. 2010.** Sequencing technologies-the next generation. *Nature reviews Genetics*
439   **11:**31-46. DOI 10.1038/nrg2626.

440 **O'Connell RJ, Thon MR, Hacquard S, Amyotte SG, Kleemann J, Torres MF, Damm U,**
441   **Buiate EA, Epstein L, and Alkan N. 2012.** Lifestyle transitions in plant pathogenic
442   *Colletotrichum* fungi deciphered by genome and transcriptome analyses. *Nature genetics*
443   **44:**1060-1065. DOI 10.1038/ng.2372.
444 **Ogoshi A. 1987.** Ecology and pathogenicity of anastomosis and intraspecific groups of
445   *Rhizoctonia solani Kuhn. Annual review of phytopathology* **25:**125-143. DOI
446   10.1146/annurev.py.25.090187.001013.
447 **Peraza L, and Hansberg W. 2002.** *Neurospora crassa* catalases, singlet oxygen and cell
448   differentiation. *Biological chemistry* **383:**569-575. DOI 10.1515/BC.2002.058.
449 **Pfaffl MW, Tichopad A, Prgomet C, Neuvians TP. 2004.** Determination of stable
450   housekeeping genes, differentially regulated target genes and sample integrity:
451   BestKeeper-excel-based tool using pair-wise correlations. *Biotechnology Letters* **26:**509–
452   515. DOI 10.1023/B:BILE.0000019559.84305.47.
453 **Priyatmojo A, Escopalao VE, Tangonan NG, Pascual CB, Suga H, Kageyama K, and**
454   **Hyakumachi M. 2001.** Characterization of a new subgroup of *Rhizoctonia solani*
455   anastomosis group 1 (AG-1-ID), causal agent of a necrotic leaf spot on coffee.
456   *Phytopathology* **91:**1054-1061. DOI 10.1094/PHYTO.2001.91.11.1054.
457 **Qiu QS, Guo Y, Dietrich MA, Schumaker KS, Zhu JK. 2002.** Regulation of SOS1, a plasma
458   membrane Na+/H+ exchanger in Arabidopsis thaliana, by SOS2 and SOS3. *PNAS*
459   **99:**8436–8441. DOI 10.1073/pnas.122224699.
460 **Radonić A. 2004.** Guideline to reference gene selection for quantitative real-time PCR.
461   *Biochemical and Biophysical Research Communications* **313:**856–862 DOI
462   10.1016/j.bbrc.2003.11.177.
463 **Ray PD, Huang B-W, and Tsuji Y. 2012.** Reactive oxygen species (ROS) homeostasis and
464   redox regulation in cellular signaling. *Cellular signalling* **24:**981-990. DOI
465   10.1016/j.cellsig.2012.01.008.
466 **Rush M, and Lee F. 1983.** Rice sheath blight: a major rice disease. *Plant Disease* **67:**829-832.
467   DOI 10.1094/PD-67-829.
468 **Silver N, Best S, Jiang J. Thein SL. 2006.** Selection of housekeeping genes for gene expression
469   studies in human reticulocytes using real-time PCR. *BMC Molecular Biology* **7:**1-9. DOI
470   10.1186/1471-2199-7-33.
471 **Sutherland MW, Learmonth BA. 1997.** The tetrazolium dyes MTS and XTT provide new
472   quantitative assays for superoxide and superoxide dismutase. *Free Radical Research*
473   27:283–289. DOI 10.3109/10715769709065766.
474 **Tingting K, Xiaokun Z, Zenggui G, Shuo Z, Ming W, Xiaoxi W, Yanbo Z. 2013.**
475   Identification and Pathogenicity of mycelium Fusion Group of Corn sheath Blight in
476   Northeast China. *Journal of Maize Sciences* **21:**132-137. DOI
477   10.13597/j.cnki.maize.science.2013.04.002.
478 **Townsend BB, Willetts HJ. 1954.** The development of sclerotia of certain fungi. *Transactions*
479   *of the British Mycological Society* **37**:213-221. DOI org/10.1016/S0007-1536(54)80003-
480   9.

481   **Trapnell C, Pachter L, and Salzberg SL. 2009.** TopHat: discovering splice junctions with
482   RNA-Seq. *Bioinformatics* **25:**1105-1111. DOI 10.1093/bioinformatics/btp120.
483   **Trapnell C, Williams BA, Pertea G, Mortazavi A, Kwan G, Van Baren MJ, Salzberg SL,**
484   **Wold BJ, and Pachter L. 2010.** Transcript assembly and quantification by RNA-Seq
485   reveals unannotated transcripts and isoform switching during cell differentiation. *Nature*
486   *biotechnology* **28:**511-515. DOI 10.1038/nbt.1621.
487   **Turrens JF. 2003.** Mitochondrial formation of reactive oxygen species. *The Journal of*
488   *physiology* **552:**335-344. DOI 10.1113/jphysiol.2003.049478.
489   **Vandesompele J. 2002.** Accurate normalization of real-time quantitative RT-PCR data by
490   geometric averaging of multiple internal control genes. *Genome Biology* **3:**research0034.
491   DOI 10.1186/gb-2002-3-7-research0034.
492   **Veluchamy S, Williams B, Kim K, and Dickman MB. 2012.** The CuZn superoxide dismutase
493   from *Sclerotinia sclerotiorum* is involved with oxidative stress tolerance, virulence, and
494   oxalate production. *Physiological and molecular plant pathology* **78:**14-23. DOI
495   10.1016/j.pmpp.2011.12.005.
496   **Wang L, Feng Z, Wang X, Wang X, and Zhang X. 2009.** DEGseq: an R package for
497   identifying differentially expressed genes from RNA-seq data. *Bioinformatics* **26:**136-
498   138. DOI 10.1093/bioinformatics/btp612.
499   **Wang Z, Gerstein M, and Snyder M. 2009.** RNA-Seq: a revolutionary tool for transcriptomics.
500   *Nature reviews genetics* **10:**57-63. DOI 10.1038/nrg2484.
501   **YonglinW, Longyan T, Dianguang X, Steven J, Shuxiao X, Chengming T. 2016.** The
502   mitogen-activated protein kinase gene, VdHog1, regulates osmotic stress response,
503   microsclerotia formation and virulence in *Verticillium dahliae*. *Fungal Genetics and*
504   *Biology* **88:**13-23. DOI org/10.1016/j.fgb.2016.01.011.
505   **Young MD, Wakefield MJ, Smyth GK, and Oshlack A. 2010.** Gene ontology analysis for
506   RNA-seq: accounting for selection bias. *Genome biology* **11:**R14. DOI 10.1186/gb-2010-
507   11-2-r14.
508   **Zhao M, Zhang Z, Zhang S, Li W, Jeffers DP, Rong T, and Pan G. 2006.** Quantitative trait
509   loci for resistance to banded leaf and sheath blight in maize. *Crop science* **46:**1039-1045.
510   DOI 10.2135/cropsci2005.0166.
511   **Zheng A, Lin R, Zhang D, Qin P, Xu L, Ai P, Ding L, Wang Y, Chen Y, and Liu Y. 2013.**
512   The evolution and pathogenic mechanisms of the rice sheath blight pathogen. *Nature*
513   *communications* **4:**1424. DOI 10.1038/ncomms2427.

Figure 1

Three distinct stages in the formation of sclerotia of *R. solani* AG1 IA.

(A) mycelium (4 d of growth); (B) initiation(5 d of growth), and (C) maturation (7 d of growth).

Photo credit: Bo Liu.
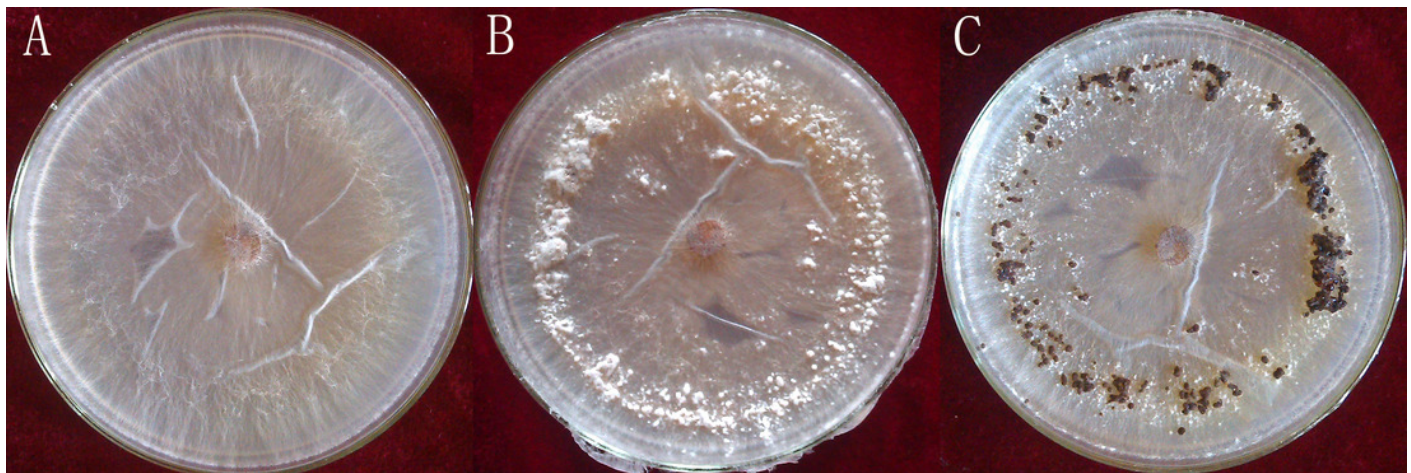
Figure 2

Bioinformatic analyses of RNA-seq data.
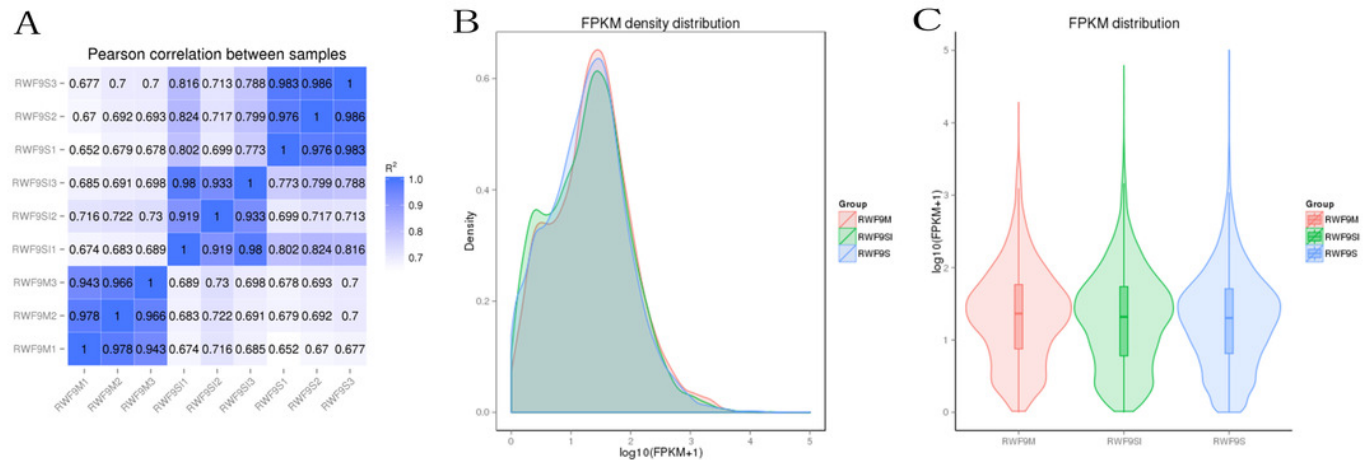
Figure 3

Differentially expressed genes analysis.

(A) Venn diagram of differentially expressed genes in the sclerotia formation of *R. solani* AG1 IA. (B-D) Volcano plot showing genes differently expressed between different libraries. The Q-value for all plots was < 0.005 and the absolute value of the $\log^2$Ratio > 1 were used as the threshold to judge the significance of the difference in gene expression. Red points: genes up-regulate; Green points: genes down-regulated; Blue points: not DEGs.

Figure 4

The difference of GO gene enrichment column, which reflects in the biological process, cellular component and molecular function.

The ordinate is the enrichment of GO term, the abscissa is the number of genes in the term. In different colors to distinguish between biological processes, cell component and molecular function.
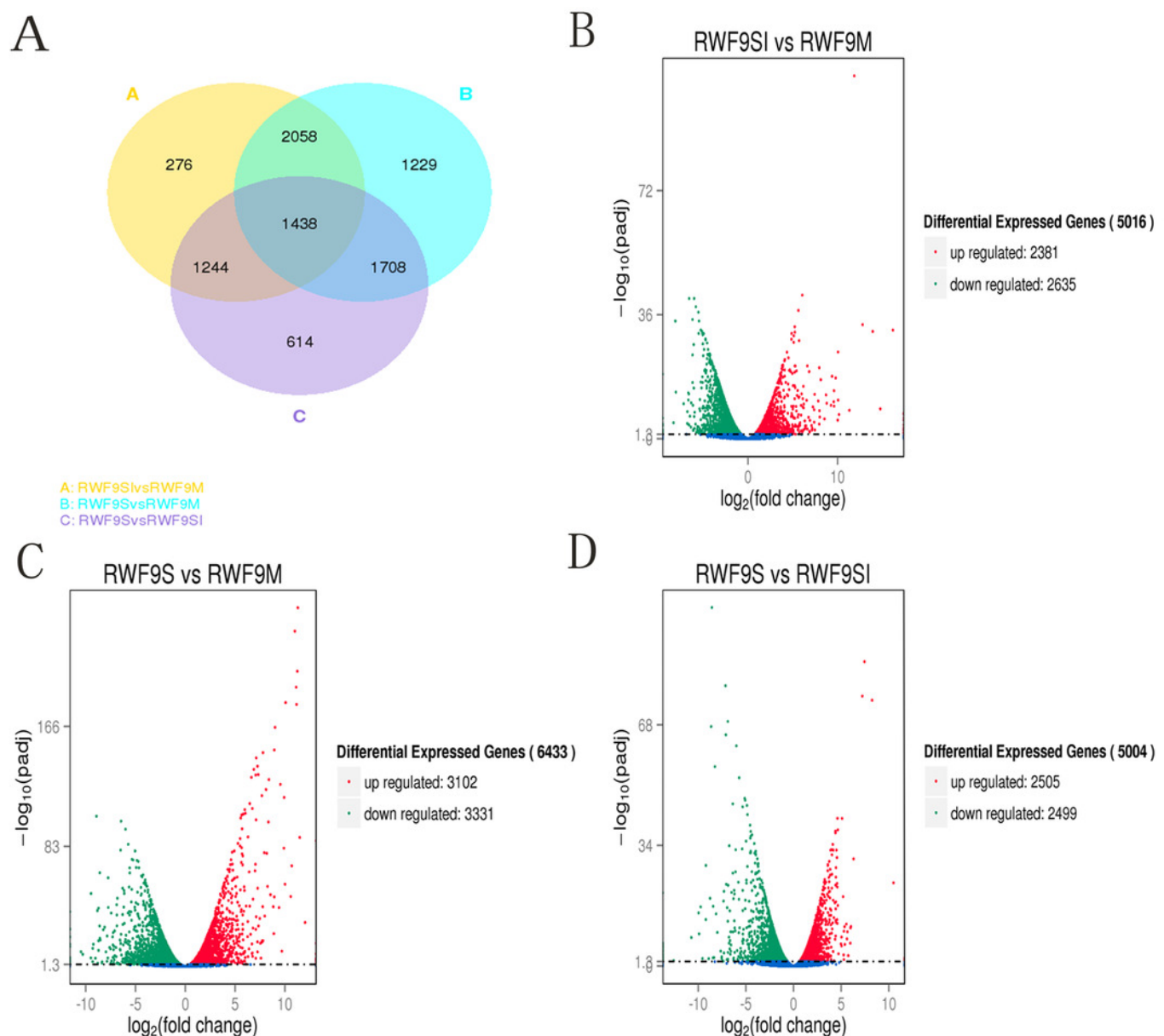
Figure 5

The clusters analysis.

(A) Expression patterns of the genes in the eight main clusters, namely subcluster 1- 8, corresponding to the heatmap.The gray is gene; The blue is gene tendency. (B) Hierarchical analysis and gene expression patterns of DEGs at three stages. Hierarchical cluster analysis of gene expression based on FPKM data. Low expression (blue) and high expression (red). The different stage is shown in the column and the transcriptional units in the rows. DEGs clustered in eight groups according to the similarity of their expression pattern.

A

subcluster_1, 2334 genes

subcluster_2, 1398 genes

subcluster_3, 220 genes

subcluster_4, 570 genes

subcluster_5, 2511 genes

subcluster_6, 922 genes

subcluster_7, 586 genes

subcluster_8, 26 genes

B

Cluster analysis of differentially expressed genes
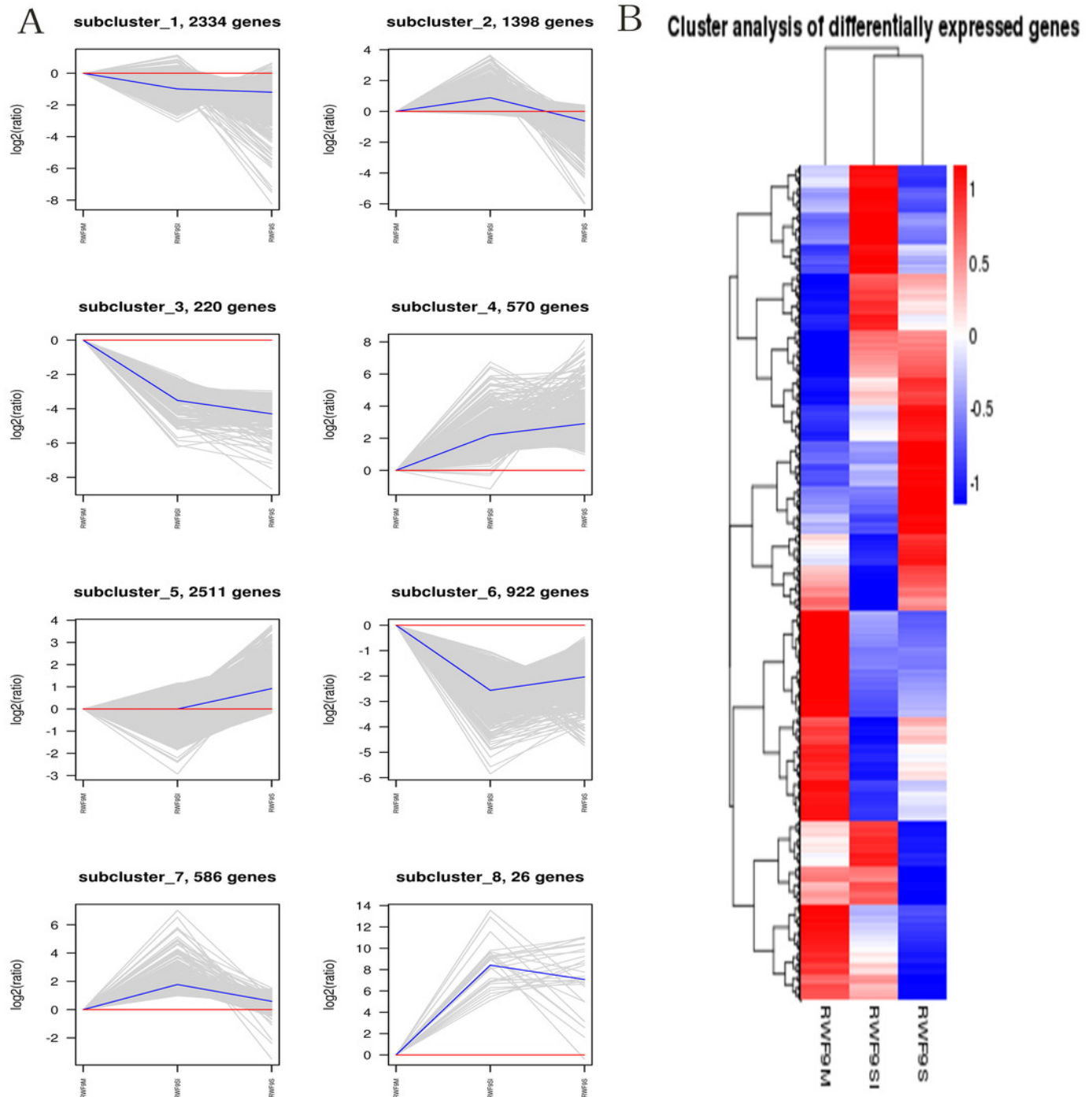
Figure 6

Oxidative stress responses

The ROS production levels and the enzyme activities of NOX1, SOD, and catalase (CAT) in three stages.M: mycelial SI: sclerotial initiation S: sclerotial maturation. (p<0.01 * p<0.05, ** p<0.01)
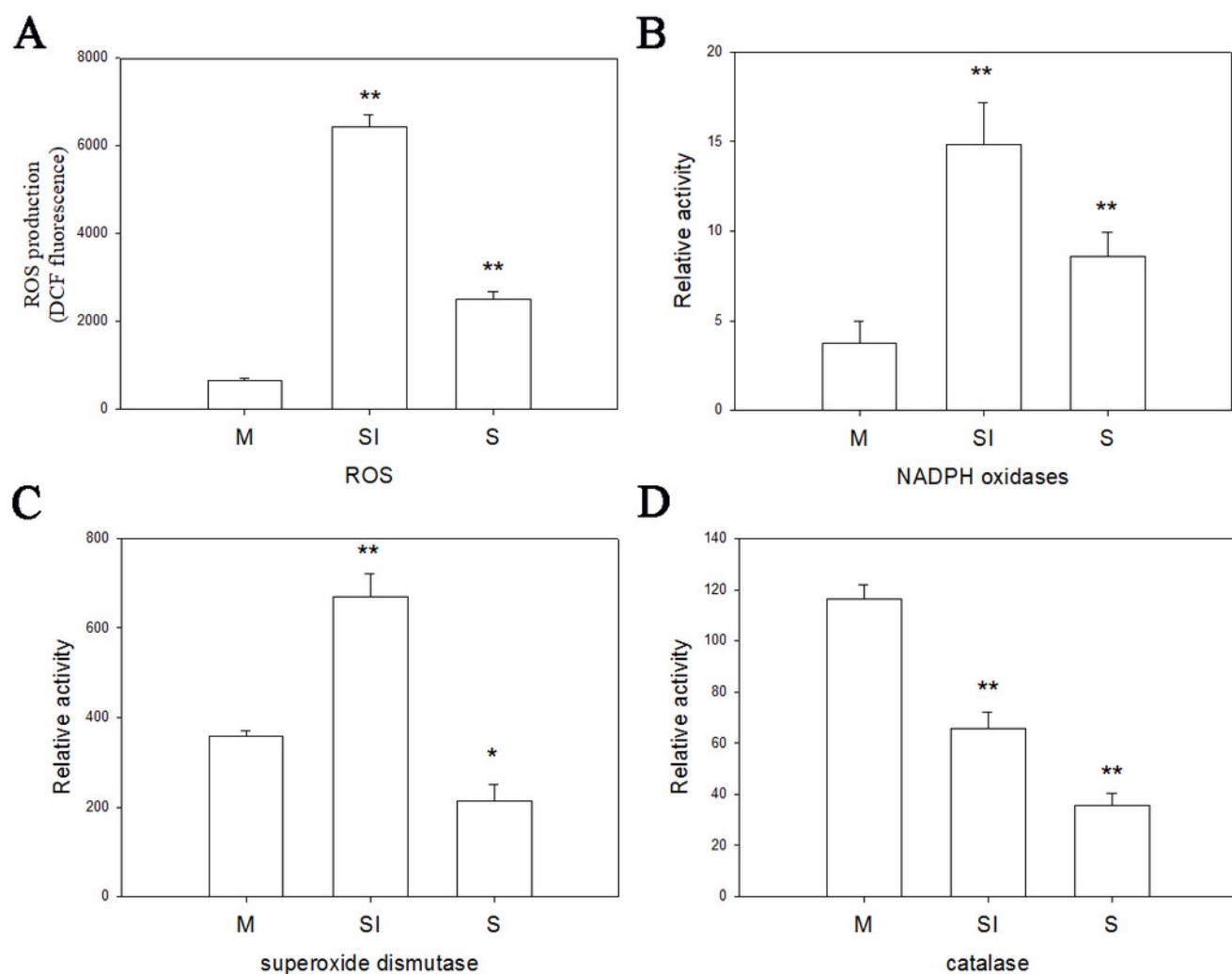
Figure 7

The expression level of twelve genes.

Real-time Quantitative PCR analysis of twelve genes in *R. solani* AG1 IA sclerotia maturation stage S1, S2, S3. S1: RWF9M S2: RWF9SI S3: RWF9S.
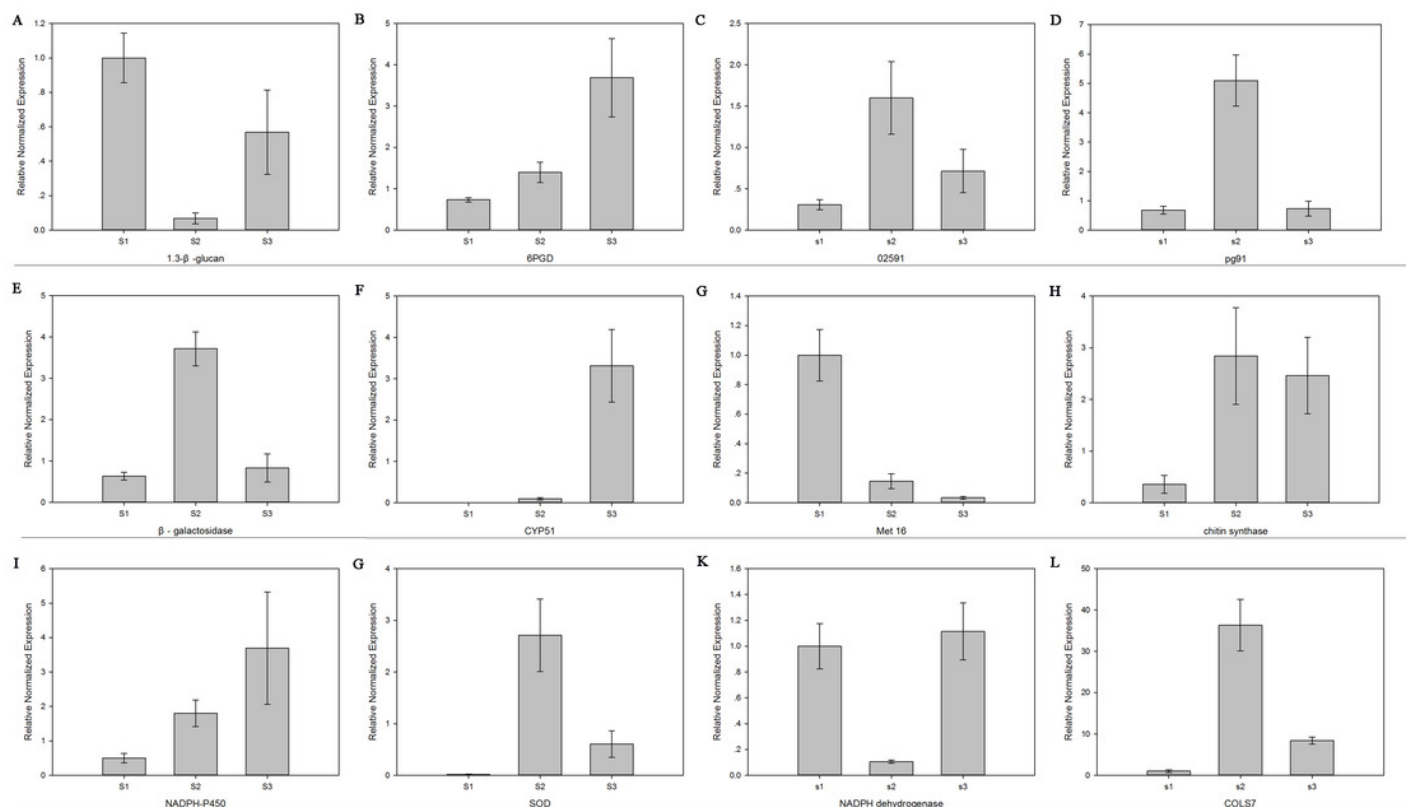
Output statistics of sequencing.

1.RWF9M1 RWF9M2 RWF9M3 three biological replicates. 2.RWF9SI1 RWF9SI2 RWF9SI3 three biological replicates. 3.RWF9S1 RWF9S2 RWF9S3 three biological replicate.

Sample name	Raw reads	Clean reads	Clean bases	Error rate (%)	Q20 (%)	Q30(%)	GC content (%)
RWF9M1	65770094	63841862	9.58G	0.02	96.92	91.97	52.55
RWF9M2	45449762	44158454	6.62G	0.02	96.98	92.04	52.51
RWF9M3	47018438	45744426	6.86G	0.01	97.12	92.35	52.20
RWF9SI1	52198062	49959440	7.49G	0.02	95.92	90.83	51.73
RWF9SI2	50834824	48902210	7.34G	0.02	96.33	91.35	52.27
RWF9SI3	49758464	47654054	7.15G	0.02	95.87	90.79	51.71
RWF9S1	54806008	53216446	7.98G	0.02	96.92	91.94	51.10
RWF9S2	52379712	50897498	7.63G	0.02	96.99	92.08	51.09
RWF9S3	59548520	57944112	8.69G	0.01	97.11	92.33	51.23

Kegg RWF9SI vs. RWF9M.

Kegg pathway	Number of Unigenes	Percentage
Metabolic pathways	454	20.77
Biosynthesis of secondary metabolites	195	8.92
Biosynthesis of amino acids	99	4.53
Ribosome	91	4.16
Carbon metabolism	84	3.84
RNA transport	49	2.24
Protein processing in endoplasmic reticulum	44	2.01
Oxidative phosphorylation	43	1.97
Spliceosome	38	1.74
Glycolysis / Gluconeogenesis	36	1.65
Cysteine and methionine metabolism	35	1.6
Arginine and proline metabolism	34	1.56
Pyruvate metabolism	34	1.56
2-Oxocarboxylic acid metabolism	32	1.46
Proteasome	31	1.42
Cell cycle – yeast	31	1.42
mRNA surveillance pathway	30	1.37
Purine metabolism	30	1.37
Glycine, serine and threonine metabolism	28	1.28
Valine, leucine and isoleucine degradation	26	1.19

Kegg RWF9S vs. RWF9M.

Kegg pathway	Number of Unigenes	Percentage
Metabolic pathways	498	21.78
Biosynthesis of secondary metabolites	219	9.58
Biosynthesis of amino acids	97	4.24
Ribosome	85	3.72
Carbon metabolism	82	3.59
RNA transport	51	2.23
Protein processing in endoplasmic reticulum	44	1.92
Glycolysis / Gluconeogenesis	42	1.84
Cell cycle – yeast	39	1.71
Oxidative phosphorylation	38	1.66
Pyruvate metabolism	37	1.62
Arginine and proline metabolism	36	1.57
Purine metabolism	34	1.49
Spliceosome	31	1.36
Cysteine and methionine metabolism	30	1.31
Glycine, serine and threonine metabolism	29	1.27
Proteasome	29	1.27
Ribosome biogenesis in eukaryotes	29	1.27
Glutathione metabolism	28	1.22
Valine, leucine and isoleucine degradation	28	1.22

Kegg RWF9S vs. RWF9SI.

Kegg pathway	Number of Unigenes	Percentage
Metabolic pathways	342	18.17
Biosynthesis of secondary metabolites	134	7.12
Ribosome	80	4.25
Biosynthesis of amino acids	55	2.92
Carbon metabolism	49	2.6
RNA transport	47	2.5
Protein processing in endoplasmic reticulum	45	2.39
Spliceosome	45	2.39
Starch and sucrose metabolism	37	1.97
Cell cycle – yeast	37	1.97
Purine metabolism	37	1.97
Pyrimidine metabolism	28	1.49
Glycolysis / Gluconeogenesis	27	1.43
Meiosis – yeast	27	1.43
mRNA surveillance pathway	26	1.38
Oxidative phosphorylation	26	1.38
Arginine and proline metabolism	25	1.33
Peroxisome	25	1.33
N-Glycan biosynthesis	23	1.22
Amino sugar and nucleotide sugar metabolism	23	1.22